Structural modification by adding Li cations into Mg/Cs-TFSA molten salt facilitating Mg electrodeposition

Koji Ohara,[a,*] Yasuhiro Umebayashi,[b] Tetsu Ichitsubo,[c] Kazuhiko Matsumoto,[d] Rika Hagiwara,[d] Hajime Arai,[a] Masahiro Mori,[a] Yuki Orikasa,[e] Shinya Okamoto,[c] Masatsugu Oishi,[f] Yuka Aiso,[d] Toshiyuki Nohira,[d] Yoshiharu Uchimoto,[e] Zempachi Ogumi,[a] and Eiichiro Matsubara[c]

[a] Office of Society-Academia Collaboration for Innovation, Kyoto University, Gokasho, Uji, Kyoto 611-0011, Japan.
[b] Graduate School of Science and Technology, Niigata University, 8050 Ikarashi 2-no-cho, Nishi-ku, Niigata City 950-2181, Japan.
[c] Department of Materials Science and Engineering, Kyoto University, Yoshida-honmachi, Sakyo-ku, Kyoto 606-8501, Japan.
[d] Graduate School of Energy Science, Kyoto University, Yoshida-honmachi, Sakyo-ku, Kyoto 606-8501, Japan.
[e] Graduate School of Human and Environmental Studies, Kyoto University, Yoshida-nihonmatsu-cho, Sakyo-ku, Kyoto 606-8501, Japan.
[f] Graduate School of Engineering, Kyoto University, Yoshida-honmachi, Sakyo-ku, Kyoto 606-8501, Japan.

*E-mail: k-ohara@saci.kyoto-u.ac.jp Phone: +85-774-38-4969

Liquid structures of Li/Mg/Cs-TFSA (TFSA: bis(trifluoromethylsulfonyl)amide, $N(SO_2CF_3)_2^-$) molten-salt systems have been investigated by Raman spectroscopy and high-energy X-ray diffraction. The Raman spectroscopic measurements indicate that the *cis*-conformer of the TFSA anion is more favorable than the *trans*-conformer in the molten salts containing Li^+ and/or Mg^{2+}, whereas the latter is dominant for a pure Cs[TFSA] molten salt. The present reverse Monte Carlo (RMC) structural modelling suggests that the coordination number of the anion around Mg, $N_{Mg\text{-}anion}$, decreased in $Li_{0.1}Mg_{0.1}Cs_{0.8}[TFSA]_{1.1}$ molten salt compared to that in $Mg_{0.1}Cs_{0.9}[TFSA]_{1.1}$. The Mg-anion distance under the coexistence of Li^+ is found to be about 10-15 % longer than that without Li^+ at around $N_{Mg\text{-}anion} \sim 1.5$, which means the increase of free volume around Mg cations in the Li-contained molten salt. Thus, the electrodeposition of Mg in alkali-TFSA molten salts would be facilitated under the coexistence of Li cations.

Grapical Abstract Text and Figure.

Free volume around Mg ions in Li/Mg/Cs-TFSA by adding Li cations has been studied by Raman spectroscopy and high-energy X-ray diffraction, which would facilitate the Mg electrodeposition, which has been studied by Raman spectroscopy, high-energy X-ray diffraction, and reverse Monte Carlo structural refinement using molecular mechanics.

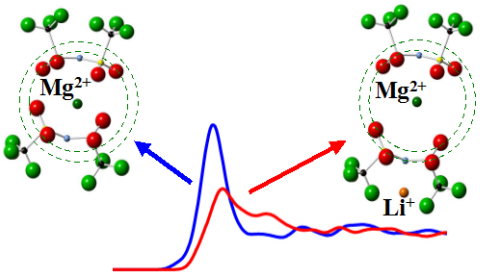

Keywords

Liquid structure; molten salts; Free volume; Raman spectroscopy; High energy X-ray diffraction;

Introduction

Molten salts consisting of alkali cations and halide anions are excellent candidates as safe electrolytes owing to their prominent properties, such as, low flammability, negligible vapour pressure, good thermal and electrochemical stability, and high ionic conductivity.[1] For the realisation of commercial products, room-temperature molten salts have been applied to lithium ion batteries.[2-6] Molten salts consisting of alkali cations and bis(trifluoromethylsulfonyl)amide (TFSA) anions have attracted attention[6-8] because of their high conductivity, and can be used as electrolytes at the intermediate temperature range (373 to 473 K).[9, 10] Such moderate temperatures enable the application of the molten salts to battery electrolytes and are favorable for the durability of battery components, such as the current collector and case material, compared with those of high-temperature molten salts. To clarify the origin of the low melting point and the chemical stability, the structure and dynamics of the TFSA molten salts have been explored well.[11-14] Theoretical approaches to elucidate these characteristics are also reported.[15-21] Recently, the successful Mg electrodeposition by adding Li^+ in the TFSA molten salt is reported as well as the high safety and the outstanding electrochemical characteristics of Mg ion batteries. [22, 23] A plausible structure model is required to examine the structural modification by adding Li^+ in alkali-TFSA molten salts, due to the lack of information on the coordination environment of Mg^{2+}.

Diffraction experiments are powerful methods of analyzing the structure of not only crystalline materials but also disordered materials such as glass, liquids, and amorphous solids. X-ray and neutron diffractions have been widely used to determine coordination numbers and bond lengths. These can be obtained by Fourier transformation for a total structure factor to the real-space pair distribution function. A structural analysis for Li[TFSA] comprising a combination of high-energy X-ray diffraction and MD simulation was reported.[17] The results suggest long-range anion–anion correlations caused by the formation of TFSA anion clusters around Li^+ ions. The complexity of the molecular structure of the TFSA anion makes such diffraction analysis difficult. Furthermore, it is well known that two kinds of conformers exist for the TFSA anion in alkylimidazolium

TFSA,[24] 1-butyl-3-methylimidazolium TFSA,[25] and 1-ethyl-3-methylimidazolium TFSA.[26] Raman spectroscopy is utilized as a complementary technique for structural analysis of the TFSA anion.

Reverse Monte Carlo (RMC) simulation is a convenient tool for modeling liquid structures obtained by diffraction techniques and makes it possible to generate a three-dimensional structural model for glass, liquids, and amorphous materials from diffraction data without using interatomic potentials.[27-30] However, a technical problem in RMC is how to constrain the intra-molecular configuration in complicated systems such as ionic liquids. Recently, new codes for RMC have been developed to solve this problem, wherein the dihedral potential can be treated restrictively,[31] and to deal with the intra-molecular flexibility by molecular mechanics (RMC-MM).[32] In the RMC-MM simulation, the intra-molecular structure is constrained by the MM, whereas the inter-molecular structure is modeled by the usual RMC simulation using the experimental diffraction data. Although an interaction has been suggested by structural models based on the molecular orbital calculation in many cases,[16, 17, 33, 34] this method enables the structural refinement between ions of complicated molten salts on the basis of experimental diffractions on a much larger scale than in that in theoretical orbital calculation.

The final goal of our study is to understand the relationship between structural properties and physicochemical characteristics by revealing the interactions between ions, in order to contribute to the development of high-performance batteries. In this study, structural models with two kinds of conformers in the TFSA anion are demonstrated by RMC-MM simulation with the aid of Raman spectroscopy, which are more plausible structures than those obtained by X-ray diffraction only. We target $Mg[TFSA]_2$ - M[TFSA] (M = Cs, Li) molten salts in which the electrodeposition of Mg by adding Li^+ [22, 23] has been found, which is very important in understanding the relationship between liquid structure and electrodeposition of Mg. The structural modification in alkali molten salts containing Li^+ and/or Mg^{2+} is evaluated from the structural model, reproducing the experimental results of Raman spectroscopy and high-energy X-ray diffraction well.

Results and discussion

To quantitatively reproduce *cis*- and *trans*-conformers of the TFSA anion, the Raman spectra of the alkali TFSA molten salts in the frequency range of 360 – 480 cm^{-1} were obtained, as shown in Fig. 1. On the basis of the Raman spectra in 1-ethyl-3-methylimidazolium [EMI][TFSA], we assigned Raman bands at approximately 400 cm^{-1} to *cis*- and *trans*-conformers for the TFSA anion.[34] The ratios of the *cis*- and *trans*-conformers were estimated and summarized in Table 1. It is quite obvious that the *cis*-conformers increase relatively to the *trans*-conformers in the alkali TFSA molten salts containing Li^+ and/or Mg^{2+} ions, which is consistent with the results of Raman spectroscopy for 1-butyl-3-methylimidazolium TFSA ($[C_4mIm]^+[TFSA]^-$).[25, 35] This increase of *cis*-conformers occurs with the reduction in the ionic radii of alkali metal ions in the salt. It is suggested that the *cis*-TFSA anion is favored in the first solvation sphere of the Li ion with a relatively small ionic radius.[35] Fujii et al. also reported that the dipole moment of the *cis*-conformer is significantly larger than that of the trans-one, implying that the *cis* geometry is preferred around the small cation.[36] Since Li^+ and Mg^{2+} possess similar ionic radii, the surrounding TFSA anions take the *cis*-conformation as a result of the increase in Li[(*cis*-)TFSA] and Mg[(*cis*-)$TFSA]_2$ in this ternary system.

Figure 2 shows the structure factors, $S(Q)$, for the alkali TFSA molten salts up to Q = 20 $Å^{-1}$. The oscillations remain to the high-Q region in all molten salts. Since the oscillations of the high-Q region are expressed for the correlation of the short distance, the structure contains many covalent bonds. This is often the case when ions such as TFSA anions exist in the system. The profile similarity in this region suggests that the intra-molecular structure of the molten salts is unchanged, as shown in an earlier study.[34] Furthermore, the oscillations of the low-Q region expressing the long-range correlations are also unchanged. The pre-peak at around Q = 0.6 $Å^{-1}$ already present in the pure Cs[TFSA], which suggests the correlation between same ionic species ions (*i.e.* between Cs ions) appear at a longer distance. The total pair distribution function, $g(r)$, for the alkali TFSA

molten salts derived by the Fourier transformation of the experimental $S(Q)$, as shown in Fig. S1. Here, we carried out the RMC-MM structural modeling for the observed $S(Q)$, fixing the ratios of *cis*- and *trans*-conformers on the basis of Raman spectroscopy measurements to reproduce the plausible liquid structure.

The total structure factors $S(Q)$ of the alkali TFSA molten salts derived from the RMC-MM model are shown in Fig. 2 as lines. It was confirmed that the RMC-MM models are consistent with the experimental data. The partial pair distribution functions (PDFs), $g_{ij}(r)$, for the alkali TFSA molten salts were calculated from the RMC-MM models. Figure S2 shows the intra-molecular $g_{ij}(r)$ of the TFSA anion, which consists of the first neighbor covalent bond (see the schematic in Fig. S2(f)). The restraint for *cis*- and *trans*-conformers is functioning well, as shown by the RMC-MM simulation. The slight difference is observed in $Li_{0.1}Mg_{0.1}Cs_{0.8}[TFSA]_{1.1}$. However, as mentioned above, the oscillations in the high-Q region remaining on the structure factors at all compositions indicate the contribution of the intra-molecular atom-atom correlations is not affected by the ratio of cations.

The three-dimensional structural model for the alkali TFSA molten salts is obtained by RMC-MM modeling. To evaluate this model in detail, we calculated PDFs for A-N (A; Li, Mg, Cs) as the general form of $g(r)$ and show the results in Fig. 3. We assume the N to representative anion here. The $g(r)$ for the Mg-N correlation, $g_{Mg\text{-}N}(r)$, has a short correlation distance of 3.3 Å compared with those of $g_{Li\text{-}N}(r)$ and $g_{Cs\text{-}N}(r)$ (Figs. 3(a), (b), and (c)). This means Mg^{2+} attracts the TFSA anion strongly compared with Cs^{+}. The $g_{Mg\text{-}O}(r)$ also shows this feature, whereas $g_{Mg\text{-}F}(r)$ does not have the strong correlation (Figs. S4(d) and (g)). Furthermore, the length of $g_{Cs\text{-}N}(r)$ became short by adding Li^{+} or/and Mg^{2+}, as shown in Fig. 3(c). This is consistent with the composition dependence of *cis*- and *trans*-conformers in the TFSA anion. Strangely, there was no characteristic peak in $g_{Li\text{-}N}(r)$, as shown in Fig. 3(b), although we expected a strong correlation. Regarding $g_{Mg\text{-}N}(r)$ shown in Fig. 3(a), it was confirmed that correlations become weak on introducing Li^{+}. To understand the coordination environment of Mg in detail, we calculated the

bond distance to the coordination number of the anion around Mg, $N_{Mg\text{-}N}$, as shown in Fig. 4(a). The maximum coordination number of 2.0 was determined from the valence of Mg. Intriguingly, the Mg-N distance in $Li_{0.1}Mg_{0.1}Cs_{0.8}[TFSA]_{1.1}$ is found to be approximately 10-15 % longer than that in $Mg_{0.1}Cs_{0.9}[TFSA]_{1.1}$ at around $N_{Mg\text{-}N}$ ~ 1.5., which suggests that the free volume around Mg ions increases by adding Li^+ in the system. Actually, the atomic number density of $Li_{0.1}Mg_{0.1}Cs_{0.8}[TFSA]_{1.1}$ (0.0568 $Å^{-3}$) is smaller than that of $Mg_{0.1}$ $Cs_{0.9}[TFSA]_{1.1}$ (0.0571 $Å^{-3}$), as shown in Table 1. This may be closely related to the successful electrodeposition of Mg in the ternary $Li_pMg_qCs_r[TFSA]_{p+2q+r}$ system.[22, 23] To obtain statistical details regarding the distribution of the anion around Mg^{2+}, the distributions of the Li-N and Mg-N correlations were calculated, as shown in Fig. 5. Since the integral maximum distance was set to 4.0 Å, the zero of the coordination number exists. As can be seen in this figure, the coordination number of Mg^{2+} decreases in $Li_{0.1}Mg_{0.1}Cs_{0.8}[TFSA]_{1.1}$ compared to that in $Mg_{0.1}Cs_{0.9}[TFSA]_{1.1}$; however it is still larger than that of Li^+. This feature is consistent with the results in the previous study, which suggested the formation of clusters of two TFSA anions around Li^+ ion.[17] The distribution of the Cs-N correlation is unchanged in these compositions, as shown in Fig. S5. Fig. 4(b) shows a schematic illustration of the coordination environment around Mg^{2+} in $Mg_{0.1}Cs_{0.9}$ $[TFSA]_{1.1}$. The inside dashed line of 4.0 Å indicates the Mg-N distance at around $N_{Mg\text{-}N}$ ~ 1.5 in $Mg_{0.1}Cs_{0.9}[TFSA]_{1.1}$, whereas that in $Li_{0.1}Mg_{0.1}Cs_{0.8}[TFSA]_{1.1}$ becomes 4.4 Å, as shown in Fig. 4(c). It is worth mentioning that the free volume around Mg^{2+} is extended approximately 37.8 % as the volume. Such increase of free volume around Mg^{2+} is induced by the addition of Li^+. This suggests that the coexistence of Li^+ facilitates the electrodeposition of Mg in alkali-TFSA molten salts. The small Li+ cations would attract TFSA anions strongly compared to large Cs^{2+} cations due to their high surface density of charges, which may enlarge the free volume around Mg^{2+} cations. Thus, the coexistence of such cations of different ionic radii and charges would facilitate the magnesium electrodeposition, which contributes to the development of high-performance batteries.

Conclusion

From the Raman spectroscopy measurement, the increase of the *cis*-TFSA anion is observed in $Li_pMg_qCs_r[TFSA]_{p+2q+r}$ molten salts containing Li^+ and/or Mg^{2+} ions, which is consistent with the earlier works.[17] The present reverse Monte Carlo structural refinements using molecular mechanics (RMC-MM) simultaneously reproduce high-energy X-ray diffraction data and Raman spectroscopic results, quantitatively fixing two kinds (*cis* and *trans*) of conformers in the TFSA anion. The plausible RMC structures indicate the coordination number of the anion around Mg^{2+}, $N_{Mg\text{-}N}$, decreased in $Li_{0.1}Mg_{0.1}Cs_{0.8}[TFSA]_{1.1}$ molten salt compared to that in $Mg_{0.1}Cs_{0.9}[TFSA]_{1.1}$. It is emphasized here that the Mg-anion distance under the coexistence of Li^+ is approximately 10-15 % longer than that without Li^+ at around $N_{Mg\text{-}N}$ ~ 1.5, and thus the coexistence of Li^+ can increase the free volume around Mg^{2+} in the TFSA molten salts, which would facilitate the Mg electrodeposition. Actually, it is already reported that Mg metal can be electrodeposited in the TFSA molten salts containing Li^+ and/or Mg^{2+}.[22, 23] Therefore, our present finding is a considerably important concept in the TFSA molten salts, and would lead to further understanding of the correlation between their structures and electrochemical behaviors.

EXPERIMENTAL METHODS

Samples were prepared as described previously.[9] Raman spectra were obtained at 443 K using the 633 nm line of a He-Ne laser as the excitation line (Nanofinder 30, Tokyo Instrument). The sample was loaded in a Ni open cell that was placed in an air tight heating stage (10042, Japan High Tech Co., Ltd.) under dry Ar atmosphere. On the basis of the previous work,[25, 36] the ratio of *cis*- and *trans*-conformers in the TFSA anion was determined from the intensities of two peaks (*cis*- and *trans*-conformers correspond to the peaks at high and low frequencies, respectively) at approximaltely 400 cm^{-1} in the observed Raman spectra. The Raman peaks were assumed to be represented as a Lorentzian function and their positions were not fixed during fitting.

The high-energy X-ray diffraction experiments for molten salts $Li_pMg_qCs_r[TFSA]_{p+2q+r}$ (*p*, *q*, *r*: 0.0, 0.0, 1.0; 0.0, 0.1, 0.9 and 0.1, 0.1, 0.8) were carried out at 438 K within 5 K at the SPring-

8 BL04B2 beamline using a two-axis diffractometer.[37] The incident X-ray energy obtained from a Si 111 crystal monochromator was 113 keV. The diffraction patterns of the sample and an empty capillary were measured in the transmission geometry. The intensity of incident X-ray was monitored in an ionization chamber filled with Ar gas and the scattered X-rays were detected by a Ge detector. A vacuum electric chamber was used to suppress air scattering around the sample. The collected datasets were corrected for the absorption, background, and polarization effects. The details of data correlation and normalization procedures are given in ref. 37.

COMPUTATIONAL METHOD

The molecular mechanics (MM) procedure was performed by employing the widely used TINKER code.[38-40] The total potential energy is given in the following equation as a sum of the potential energy of each molecule:

$$E_{\text{molecule}} = \Sigma E_{\text{bond}} + \Sigma E_{\text{angle}} + \Sigma E_{\text{torsion}},$$

where E_{bond} is the bond energy, E_{angle} is the energy of the angle, and E_{torsion} is the energy of the torsion in the molecule. Before analyzing the inter-molecular correlations in detail, it is of primary importance to reproduce the intra-molecular geometries in the TFSA anion using the results of Raman spectroscopic results listed in Table 1. These geometries are realised by using the following equation of torsion energy:

$$E_{\text{torsion}} = K (1 + \cos(n \varphi - \varphi_0)),$$

where K is the force constant, n is the number of the symmetry, φ is the dihedral angle, and φ_0 is the initial phase. We selected 2 and 90 for n and φ_0, respectively, which realise the dihedral angle of 0° and 180° for the *cis*- and *trans*-conformers, respectively, in the TFSA anion.

In our RMC-MM simulations, the total number of alkali TFSA molten salts was 500 cation-anion pairs. It was 8750 atoms when Mg^{2+} ion was present, and 8000 atoms when absent. To obtain a plausible structural model, we checked the densities (Fig. S6). The initial configurations were prepared by arranging the cation-anion pairs randomly in a cubic box with corresponding densities

as listed in Table 1. The cut-offs, *i.e.*, the minimum allowed distances between atom pairs, were estimated from the experimental pair distribution function. The force-field parameters for the alkali TFSA molten salts were taken from the parameters given in ref. 41. The simulations were performed for four different initial configurations for each composition, and the validities were checked.

Table

Table 1. Details of alkali TFSA molten salts; compositions, densities, atomic number densities, particle numbers for RMC simulation, and the ratios of *cis*- and *trans*-conformers.

Li, Mg, Cs	0.0, 0.0, 1.0	0.0, 0.1, 0.9	0.1, 0.1, 0.8
Composition	$[Cs^+]_{1.0}$ $[N(SO_2CF_3)_2^-]_{1.0}$	$[Mg^{2+}]_{0.1}[Cs^+]_{0.9}$ $[N(SO_2CF_3)_2^-]_{1.1}$	$[Li^+]_{0.1}[Mg^{2+}]_{0.1}[Cs^+]_{0.8}$ $[N(SO_2CF_3)_2^-]_{1.1}$
Density (g/cm^3)	2.39	2.33	2.25
Atomic number density ($Å^{-3}$)	0.0558	0.0571	0.0568
Ratio of *cis* and *trans*	20 : 80	66 : 34	79 : 21
Particle number	8000	8750	8750
Box length ($Å^3$)	52.35	53.52	53.61

Figures

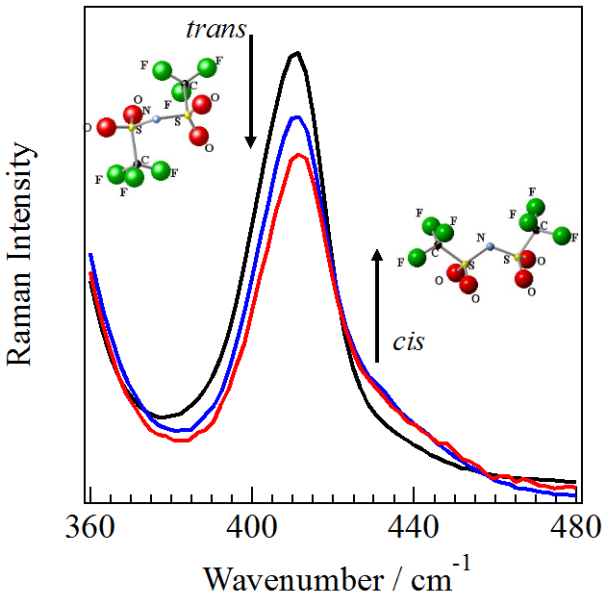

Figure 1. Raman spectra in the range 360-480 cm^{-1} for alkali TFSA molten salts.
Black, blue, and red lines represent *p*, *q*, *r* = 0.0, 0.0, 1.0; 0.0, 0.1, 0.9 and 0.1, 0.1, 0.8 of $Li_pMg_qCs_r[TFSA]_{p+2q+r}$, respectively.

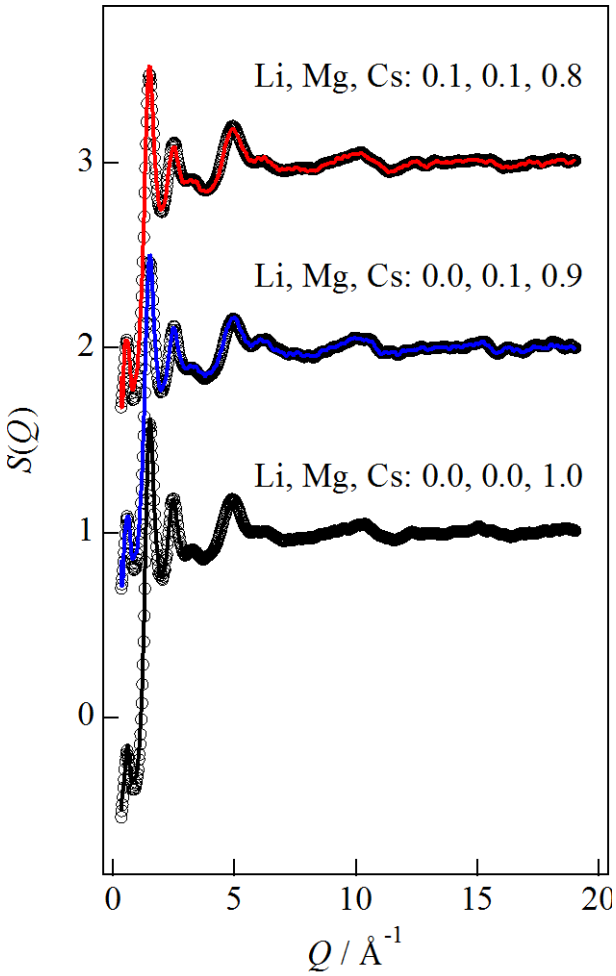

Figure 2. Total X-ray structure factors $S(Q)$ at 438 K for alkali TFSA molten salts for the Q range of $0 < Q < 20$. Circles, experimental data; lines, the RMC-MM models. Line colours correspond to those in Figure 1.

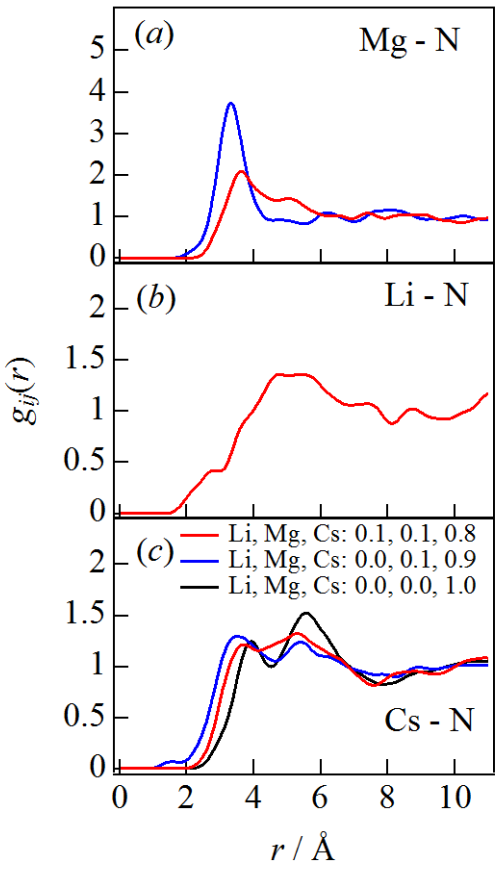

Figure 3. Pair distribution functions, $g(r)$, for Mg-N (a), Li–N (b), and Cs–N (c) derived using the RMC-MM models for alkali TFSA molten salts. Line colours correspond to those in Figure 1.

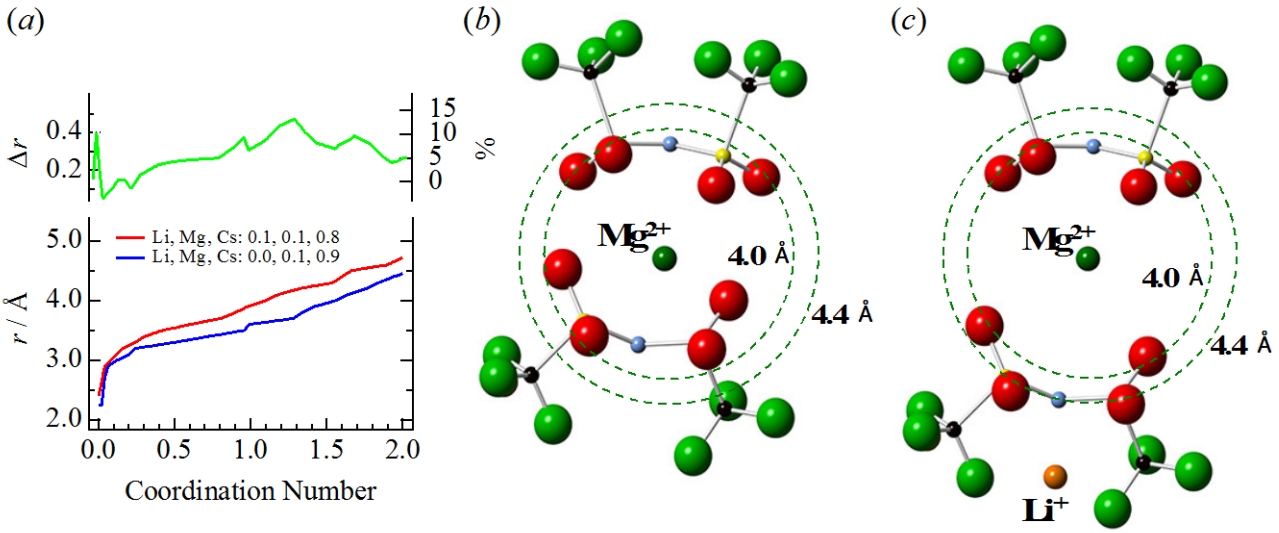

Figure 4. Bond distances for the Mg-N correlation derived using the RMC-MM models based on the valence compensation of Mg^{2+}, and their difference is shown to the upper part (a). Schematic illustrations of TFSA anions around Mg^{2+} for $Mg_{0.1}Cs_{0.9}[TFSA]_{1.1}$ (b) and $Li_{0.1}Mg_{0.1}Cs_{0.8}[TFSA]_{1.1}$ (c) which satisfied the coordination number of 1.5 for Mg-N correlation.

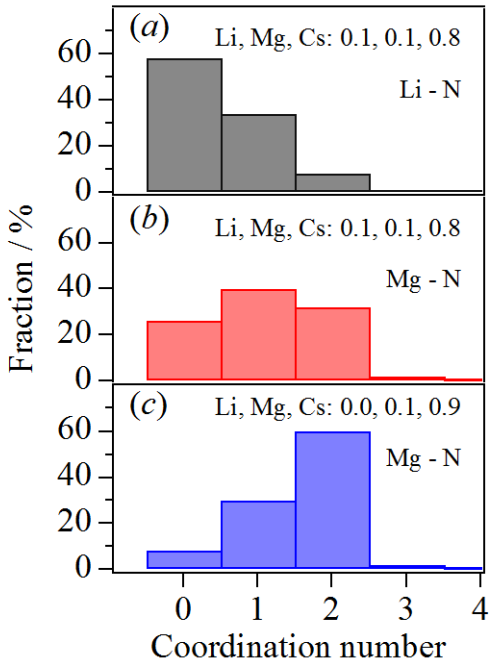

Figure 5. Coordination number statistics for alkali TFSA molten salts obtained using the RMC-MM model. Normalized fractions of Li – N (a) and Mg – N (b) coordination numbers within 4.0 Å.

Acknowledgements

The authors appreciate Dr. Hidetoshi Morita, AdvanceSoft Corporation, for his kind assistance with the RMC-MM simulation. The authors are thankful to Dr. Kenta Fujii, Yamaguchi University, for his dedicated support. This work was partially supported by the Research and Development Initiative for Scientific Innovation of New Generation Batteries (RISING) project of the New Energy and Industrial Technology Development Organization (NEDO) in Japan. The synchrotron radiation experiment was approved by the Japan Synchrotron Radiation Research Institute (proposals. 2012A1413, 2012A1669, 2012A1682, 2013A7600, and 2013B1009).

ASSOCIATED CONTENT

Electronic supplementary information (ESI) available: Detailed information concerning data analysis, extra experimental data, and associated references are available.

AUTHOR INFORMATION

Corresponding Authors
*E-mail: k-ohara@saci.kyoto-u.ac.jp

Author Contributions
The manuscript was written through contributions of all authors; K.O., R.H., H.A., Y.Uc., and E.M. designed this research; S.O., Y.A. and Y.O. prepared samples; K.O., M.M., S.O., and M.O. performed high-energy X-ray measurements; K.M., Y.A., and T.N. performed Raman spectroscopic measurements; K.O. and M.M. carried out RMC-MM simulations; K.O., Y.Um., T.I. and K.M., analyzed the data; K.O., Y. Um. T.I. K.M., R.H. and E.M. contributed to discussions of the results; K.O., Y.Um., T.I., K.M., R.H., and H.A. wrote the paper with help from all authors.

REFERENCES

1. Ito, Y. and Nohira, T., Non-conventional electrolytes for electrochemical applications, *Electrochim. Acta*, 2000**, 45**, 2611-2622.
2. Sakaebe, H. and Matsumoto, H., N-Methyl-N-propylpiperidinium bis(trifluoromethanesulfonyl)imide (PP13–TFSI) – novel electrolyte base for Li battery, *Electrochem. Commun.*, 2003**, 5**, 594-598.
3. Nakagawa, H.; Izuchi, S.; Kuwana, K.; Nukuda, T. and Aiharaz, Y., Liquid and Polymer Gel Electrolytes for Lithium Batteries Composed of Room-Temperature Molten Salt Doped by Lithium Salt, *J. Electrochem. Soc.*, 2003**, 150**, A695-A700.
4. Garcia, B.; Lavallée, S.; Perron, G.; Michot, C. and Armand, M., Room temperature molten salts as lithium battery electrolyte, *Electrochim. Acta.*, 2004**, 49**, 4583-4588.
5. Sakaebe, H.; Matsumoto, H. and Tatsumi, K., Application of room temperature ionic liquids to Li batteries, *Electrochim. Acta.*, 2007**, 53**, 1048-1054.
6. Armand, M.; Endres, F.; MacFarlane, D. R.; Ohno, H. and Scrosati, B., ionic-liquid materials for the electrochemical challenges of the future, *Nat. Mater.*, 2009**, 8**, 621-629.
7. Kubota, K. and Matsumoto, H., Investigation of an Intermediate Temperature Molten Lithium Salt Based on Fluorosulfonyl(trifluoromethylsulfonyl)amide as a Solvent-Free Lithium Battery Electrolyte, *J. Phys. Chem. C*, 2013**, 117**, 18829-18836.
8. Watarai, A.; Kubota, K.; Yamagata, M.; Goto, T.; Nohira, T.; Hagiwara, R.; Ui, K. and Kumagai, N., A rechargeable lithium metal battery operating at intermediate temperatures using molten alkali bis(trifluoromethylsulfonyl)amide mixture as an electrolyte, *J. Power Sources*, 2008**, 183**, 724-729.
9. Hagiwara, R.; Tamaki, K.; Kubota, K.; Goto, T. and Nohira, T., Thermal Properties of Mixed Alkali Bis(trifluoromethylsulfonyl)amides, *J. Chem. Eng. Data*, 2008**, 53**, 355-358.
10. Kubota, K.; Tamaki, K.; Nohira, T.; Goto, T. and Hagiwara, R., Electrochemical properties of alkali bis(trifluoromethylsulfonyl)amides and their eutectic mixtures, *Electrochim. Acta.*, 2010**, 55**, 1113-1119.
11. Johansson, P.; Gejji, S. P.; Tegenfeldt, J. and Lindgrena, J., The imide ion: potential energy surface and geometries, *Electrochim. Acta.*, 1998**, 43**, 1375-1379.
12. Herstedt, M.; Smirnov, M.; Johansson, P.; Chami, M.; Grondin, J.; Servant, L. and Lassègues, J. C., Spectroscopic characterization of the conformational states of the bis(trifluoromethanesulfonyl)imide anion (TFSI−), *J. Raman Spectrosc.*, 2005**, 36**, 762-770.
13. Herstedt, M.; Henderson, W. A.; Smirnov, M.; Ducasse, L.; Servant, L.; Talaga, D. and Lassègues, J. C., Conformational isomerism and phase transitions in tetraethylammonium bis(trifluoromethanesulfonyl)imide Et4NTFSI, *J. Mol. Struct.*, 2006**, 783**, 145-156.

14. Lassègues, J. C.; Grondin, J.; Holomb, R. and Johansson, P., Raman and ab initio study of the conformational isomerism in the 1-ethyl-3-methyl-imidazolium bis(trifluoromethanesulfonyl)imide ionic liquid, *J. Raman Spectrosc.*, 2007**, 38**, 551-558.
15. Gejji, S. P.; Suresh, C. H.; Babu, K. and Gadre, S. R., Ab Initio Structure and Vibrational Frequencies of (CF3SO2)2N-Li+ Ion Pairs, *J. Phys. Chem. A*, 1999**, 103**, 7474-7480.
16. Tsuzuki, S.; Hayamizu, K.; Seki, S.; Ohno, Y.; Kobayashi, Y. and Miyashiro, H., Quaternary Ammonium Room-Temperature Ionic Liquid Including an Oxygen Atom in Side Chain/Lithium Salt Binary Electrolytes: Ab Initio Molecular Orbital Calculations of Interactions between Ions, *J. Phys. Chem. B*, 2008**, 112**, 9914-9920.
17. Umebayashi, Y.; Hamano, H.; Seki, S.; Minofar, B.; Fujii, K.; Hayamizu, K.; Tsuzuki, S.; Kameda, Y.; Kohara, S. and Watanabe, M., Liquid Structure of and Li+ Ion Solvation in Bis(trifluoromethanesulfonyl)amide Based Ionic Liquids Composed of 1-Ethyl-3-methylimidazolium and N-Methyl-N-propylpyrrolidinium Cations, *J. Phys. Chem. B*, 2011**, 115**, 12179-12191.
18. Borodin, O.; Smith, G. D. and Henderson, W., Li+ Cation Environment, Transport, and Mechanical Properties of the LiTFSI Doped N-Methyl-N-alkylpyrrolidinium+TFSI- Ionic Liquids, *J. Phys. Chem. B*, 2006**, 110**, 16879-16886.
19. Borodin, O. and Smith, G. D., Structure and Dynamics of N-Methyl-N-propylpyrrolidinium Bis(trifluoromethanesulfonyl)imide Ionic Liquid from Molecular Dynamics Simulations, *J. Phys. Chem. B*, 2006**, 110**, 11481-11490.
20. Monteiro, M. J.; Bazito, F. F. C.; Siqueira, L. J. A.; Ribeiro, M. C. C. and Torresi, R. M., Transport Coefficients, Raman Spectroscopy, and Computer Simulation of Lithium Salt Solutions in an Ionic Liquid, *J. Phys. Chem. B*, 2008**, 112**, 2102-2109.
21. Tsuzuki, S.; Kubota, K. and Matsumoto, H., Cation and Anion Dependence of Stable Geometries and Stabilization Energies of Alkali Metal Cation Complexes with FSA−, FTA−, and TFSA− Anions: Relationship with Physicochemical Properties of Molten Salts, *J. Phys. Chem. B*, 2013**, 117**, 16212-16218.
22. Gao, B.; Nohira, T.; Hagiwara, R. and Wang, Z., Electrodeposition of Magnesium in Ionic Liquid at 150-200℃, *Chap. 5.4. in Molten Salts Chemistry and Technology, by M. Gaune-Escard and G. M. Haarberg eds.*, 2014, John Wiley & Sons, Inc., Chichester.
23. Oishi, M.; Ichitubo, T.; Okamoto, S.; Toyoda, S.; Matsubara, E.; Nohira, T. and Hagiwara, R., Electrochemical Behavior of Magnesium Alloys in Alkali Metal-TFSA Ionic Liquid for Magnesium-Battery Negative Electrode, *J. Electrochem. Soc.*, 2014**, 161**, A943-A947.
24. Holbrey, J. D.; Reichert, W. M. and Rogers, R. D., Crystal structures of imidazolium bis(trifluoromethanesulfonyl)imide 'ionic liquid' salts: the first organic salt with a cis-TFSI anion conformation, *Dalton Transactions*, 2004,

2267-2271.10.1039/B405901H
25. Umebayashi, Y.; Mori, S.; Fujii, K.; Tsuzuki, S.; Seki, S.; Hayamizu, K. and Ishiguro, S., Raman Spectroscopic Studies and Ab Initio Calculations on Conformational Isomerism of 1-Butyl-3-methylimidazolium Bis-(trifluoromethanesulfonyl)amide Solvated to a Lithium Ion in Ionic Liquids: Effects of the Second Solvation Sphere of the Lithium Ion, *J. Phys. Chem. B*, 2010**, 114**, 6513-6521.
26. Choudhury, A. R.; Winterton, N.; Steiner, A.; Cooper, A. I. and Johnson, K. A., In situ crystallization of ionic liquids with melting points below -25 [degree]C, *CrystEngComm*, 2006**, 8**, 742-745.10.1039/B609598D
27. McGreevy, R. L. and Pusztai, L., Reverse Monte Carlo Simulation: A New Technique for the Determination of Disordered Structures, *Mol. Simul.*, 1988**, 1**, 359-367.
28. Keen, D. A. and McGreevy, R. L., Structural modelling of glasses using reverse Monte Carlo simulation, *Nature*, 1990**, 344**, 423-425.
29. Gereben, O.; Jóvári, P.; Temleitner, L. and Pusztai, L., A new version of the RMC++ Reverse Monte Carlo programme, aimed at investigating the structure of covalent glasses, *J. Optelect. Adv. Mater.*, 2007**, 9**, 3021-3027.
30. Mile, V.; Gereben, O.; Kohara, S. and Pusztai, L., On the structure of aqueous cesium fluoride and cesium iodide solutions: diffraction experiment, molecular dynamics simulations and reverse Monte Carlo modeling, *J. Phys. Chem. B*, 2012**, 116**, 9758-9767.
31. Gereben, O. and Pusztai, L., RMC_POT, a computer code for Reverse Monte Carlo modeling the structure of disordered systems containing molecules of arbitrary complexity, *J. Comp. Chem.*, 2012**, 33**, 2285-2291.
32. Morita, H.; Kohara, S. and Usuki, T., A new reverse Monte Carlo simulation code combined with molecular mechanics simulation (RMC-MM0 for molecular and ionic liquids, *J. Mol. Liq.*, 2009**, 147**, 182-185.
33. Bhargava, B. L.; Klein, M. L. and Balasubramanian, S., Structural Correlations and Charge Ordering in a Room-Temperature Ionic Liquid, *Chem. Phys. Chem*, 2008**, 9**, 67-70.
34. Fujii, K.; Seki, S.; Ohara, K.; Kameda, Y.; Doi, H.; Saito, S. and Umebayashi, Y., High-energy X-ray Diffraction and MD Simulation Study on the Ion-ion Interactions in 1-Ethyl-3-methylimidazolium Bis(fluorosulfonyl)amide, *J. Sol. Chem.*, 2014**, 43**, DOI: 10.1007/s10953-014-0234-8
35. Umebayashi, Y.; Yamaguchi, T.; Fukuda, S.; Mitsugi, T.; Takeuchi, M.; Fujii, K. and Ishiguro, S., Raman Spectroscopic Study on Alkaline Metal Ion Solvation in 1-Butyl-3-methylimidazolium Bis(trifluoromethanesulfonyl)amide Ionic Liquid, *ANAL. SCI.*, 2008**, 24**, 1297-1304.
36. Fujii, K.; Fujimori, T.; Takamuku, T.; Kanzaki, R.; Umebayashi, Y. and Ishiguro, S., Conformational Equilibrium of Bis(trifluoromethanesulfonyl) Imide Anion of a Room-Temperature Ionic Liquid: Raman Spectroscopic Study and DFT Calculations, *J. Phys. Chem. B*, 2006**, 110**, 8179-8183.
37. Kohara, S.; Itou, M.; Suzuya, K.; Inamura, Y.; Sakurai, Y.; Ohishi, Y. and Takata, M., Structural studies of disordered materials using high-energy x-ray

diffraction from ambient to extreme conditions *J. Phys.: Condens. Matter*, 2007**, 19**, 506101.
38. Ponder, J. W. and Richards, F. M., An Efficient Newton-like Method for Molecular Mechanics Energy Minimization of Large Molecules, *J. Comp. Chem.*, 1987**, 8**, 1016-1024.
39. Pappu, R. V.; Hart, R. K. and Ponder, J. W., Analysis and Application of Potential Energy Smoothing and Search Methods for Global Optimization, *J. Phys. Chem. B*, 1998**, 102**, 9725-9742.
40. Ren, P. and Ponder, J. W., A Polarizable Atomic Multipole Water Model for Molecular Mechanics Simulation, *J. Phys. Chem. B*, 2003**, 107**, 5933-5947.
41. Liu, H. and Maginn, E., A molecular dynamics investigation of the structural and dynamic properties of the ionic liquid 1-n-butyl-3-methylimidazolium bis(trifluoromethanesulfonyl)imide, *J. Chem. Phys.*, 2011**, 135**, 124507.